for Predicting Second Virial Coefficients," *Ind. Eng. Chem. Process Design Develop.*, **14**, 209 (1975).
Johnson, C. H. J., and T. H. Spurling, "Multipolar Third Order Non-Pairwise Additivity of Intermolecular Forces: Effects on Crystal Properties and Third Virial Coefficients," *Aust. J. Chem.*, **24**, 2205 (1971).
Kalfoglou, N. K., and J. G. Miller, "Compressibility of Gases. V. Mixtures of Spherically Symmetric Molecules at Higher Temperatures. The Helium-Argon and Helium-Tetrafluoromethane Systems," *J. Phys. Chem.*, **71**, 1256 (1967).
Kerns, W. J., R. G. Anthony, and P. T. Eubank, "Volumetric Properties of Ciclohexane Vapor," *AIChE Symposium Ser.*, **70**, 14 (1974).
Lange, H. B., Jr., and F. P. Stein, "Volumetric Behaviour of a Polar-Non-Polar Gas Mixture: Trifluoromethane-Tetrafluoromethane System," *J. Chem. Eng. Data*, **15**, 56 (1970).
Lee, R. C., and W. C. Edmister, "Compressibilities and Virial Coefficients for Methane, Ethylene, and Their Mixtures," *AIChE J.*, **16**, 1047 (1970).
Lee, S. M., P. T. Eubank, and K. R. Hall, "Truncation Errors Associated with the Virial Equation," *Fluid Phase Equilibria*, **1**, 219 (1978).
Levelt Sengers, J. M. H., Proc. Symp. Thermophys. Properties 4th, ASME, New York (1968).
Levelt Sengers, J. M. H., M. Klein, and J. S. Gallagher, "Pressure-Volume-Temperature Relationships of Gases; Virial Coefficients," *A.I.P. Handbook*, McGraw-Hill, New York (1972).
McMath, H. G., Jr., and W. C. Edmister, "The Experimental Determination of the Volumetric Properties and Virial Coefficients of the Methane-Ethylene System," *AIChE J.*, **15**, 370 (1969).
Mears, W. H., E. Rosenthal, and J. V. Sinka, "Physical Properties and Virial Coefficients of Sulfur Hexafluoride," *J. Phys. Chem.*, **73**, 2254 (1969).
Michels, A., J. C. Abels, C. A. Ten Seldam, and W. de Graaff, "Polynomial Representation of Experimental Data Application to Virial Coefficients of Gases," *Physica*, **26**, 381 (1960).
Mihara, S., H. Sagara, Y. Arai, and S. Saito, "The Compressibility Factors of Hydrogen-Methane, Hydrogen-Ethane, and Hydrogen-Propane Gaseous Mixtures," *J. Chem. Eng. Japan*, **10**, 395 (1977).
Nothnagel, K. H., D. S. Abrams, and J. M. Prausnitz, "Generalized Correlation for Fugacity Coefficients in Mixtures at Moderate Pressures," *Ind. Eng. Chem. Process Design Develop.*, **12**, 25 (1973).
Pope, G. A., P. S. Chappelear, and R. Kobayashi, "Virial Coefficients of Argon, Methane and Ethane at Low Reduced Temperatures," *J. Chem. Phys.*, **59**, 423 (1973).
Prausnitz, J. M., *Molecular Thermodynamics of Fluid-Phase Equilibria*, Prentice-Hall, Englewood Cliffs, N.J. (1969).
Present, R. D., "Nonadditive Triple-Overlap Interactions among Rare-Gas Atoms in the Thomas-Fermi-Dirac Approximation," *J. Chem. Phys.*, **47**, 1793 (1967).
Provine, J. A., and F. B. Canfield, "Isotherms for the Helium-Argon System at −130, −115, and −90°C up to 700 Atm," *Physica*, **52**, 79 (1971).
Prydz, R., and G. C. Straty, "PVT Measurements, Virial Coefficients, and Joule-Thomson Inversion Curve of Fluorine," *J. Res. Natl. Bur. Stand.*, 744, 747 (1970).
Righter, W. M., and K. R. Hall, "Optimal Truncation of the Virial Equation," *AIChE J.*, **21**, 406 (1975).
Sigmund, P. M., I. H. Silberberg, and J. J. McKetta, "Second and Third Virial Coefficients for System Tetrafluoromethane-Sulfur Hexafluoride," *J. Chem. Eng. Data*, **17**, 168 (1972).
Tarakad, R. R., and R. P. Danner, "An Improved Corresponding States Method for Polar Fluids: Correlation of Second Virial Coefficients," *AIChE J.*, **23**, 685 (1977).
Tsonopoulos, C., "An Empirical Correlation of Second Virial Coefficients," *AIChE J.*, **20**, 263 (1974).
Warowny, W., P. Wielopolski, and J. Stecki, "Compressibility Factors and Virial Coefficients for Propane, Propene and Their Mixtures by the Burnett Method," *Physica*, **91A**, 73 (1978).
Weber, L. A., "P-V-T Pressure-Volume-Temperature Thermodynamic and Related Properties of Oxygen from the Triple Point to 300 K at Pressures to 33 MN/m^2," *J. Res. Nat. Bur. Stand.*, 744, 93 (1970).

Manuscript received October 10, 1978; revision received March 7, and accepted March 21, 1979.

Effects of Acceleration, Deceleration and Particle Shape on Single-Particle Drag Coefficients in Still Air

Measurements were made of the drag coefficients of smooth solid particles moving singly through still air at Reynolds numbers in the range of 10^3 to 10^4. Spheres were observed during acceleration, deceleration and at terminal velocity. Discs were tested during acceleration and at steady velocity. Other particles in the shapes of discs, circular cylinders and rectangular parallelepipeds were tested at steady velocity in their preferred and, in some cases, non-preferred orientations. The effects of non-steady velocity and of particle form were determined. An unexpected influence of particle density was observed for some of the particles.

E. K. MARCHILDON
and
W. H. GAUVIN
Department of Chemical Engineering
McGill University,
Montreal, Quebec, Canada

SCOPE

The interaction between particles and a moving fluid forms the basis of an ever-increasing variety of operations in chemical and metallurgical processing. Processing operations may be purely physical (pneumatic conveying, settling, cyclone separation). They may involve superimposed mass transfer (spray drying, flash drying, cyclone evaporation). More recent and more exciting developments involve chemical reactions (transport reactors, rocket propulsion, combustion, reactions in plasma flames or electric

Present address for the first author is: Research Centre, Du Pont of Canada, Kingston, Ontario, Canada.

arcs, etc.). In all these systems, accurate predictions of particle trajectory and residence time (which may be as low as a few millisec in plasma systems) are necessary for design purposes or for analyzing and optimizing the system's performance. Knowledge of the particle relative velocity is also invariably required in the calculation of the heat and mass transfer rates.

Many studies have been made of freely-moving particles in liquids and of the flow of gases around fixed objects. Free particulate motion in gases has been less studied and, in many cases, either the rotational behavior of the particle or the condition of motion of the gas has been uncertain. It must be recognized that the phenomenon of fluid resistance is extremely complex; the reported measurements of the fluid drag, as expressed by the drag coefficient of the particle, have often been confusing and sometimes contradictory.

Particulate motion in gases differs from motion in liquids in some fundamental respects, owing to the large difference in density between fluid and particle in the former case, and to the difference in viscosity between the two fluids. Motion in gases is characterized by: (1) smaller drag forces than in liquids for the same relative velocity, (2) the absence of a significant added-mass effect during acceleration or deceleration, (3) smaller particle response to wake-shedding forces, (4) much longer distances of travel in non-preferred orientations, and (5) the possibility of quasi-steady behavior during orientation change (i.e., the drag force may be independent of the rate of change of orientation).

Two important conclusions of a practical nature can be drawn from some of these characteristics. The first is that, in actual operations, seldom is the particle/gas contact time long enough to let the particle reach constant velocity. Thus, the particle is constantly in a state of acceleration or deceleration relative to the fluid. Second, both the shape of the particle and its orientation are bound to have important effects on its coefficient of drag. Although it is now possible to predict particle motion under some conditions of practical interest with reasonable confidence, these two aspects still offer considerable uncertainty. This is so largely because of the considerable experimental difficulties involved in their observation and measurement. It is to these two aspects that the present study is devoted.

From the features listed above, it appears that useful data for moving particles in gases can be obtained from force measurements on fixed bodies. However, to experiment at lower Reynolds numbers (the range 10^3 to 10^4 is of particular practical interest), particle dimensions must be small, and it is convenient to work with freely-moving objects. In the present study, the time-distance history of particles in vertical motion through still air was monitored and analyzed to determine drag coefficients.

In summary, the objectives were 1) to isolate and measure the effects on particulate motion of unsteady particle velocity in a gaseous medium, and 2) to obtain fixed-orientation drag data that can be used for predicting the average force on rotating or oscillating particles in gaseous systems of practical interest.

CONCLUSIONS AND SIGNIFICANCE

From the experimental results obtained on the motion of aerodynamically smooth particles in still air in the Reynolds number range of 10^3 to 10^4, the following conclusions can be drawn:

1. For spheres, deceleration (up to 210 m/s^2) increases the drag coefficient by up to 10%, if the deceleration modulus A_c is great enough, but acceleration, up to 10 m/s^2, has no effect. For both acceleration and steady motion, if the particle specific gravity exceeds 2.0, then the drag coefficient rises, with particle density, above the standard curve. This effect was unexpected and is opposite to the effect of particle density in liquid media.

2. For discs in the face-on orientation, there is a steady decrease in drag coefficient with acceleration in the range zero to 10 m/s^2. There is also a particle density effect similar to that for spheres.

3. For discs and cylinders in the face-on orientation at steady velocity, the thickness-to-diameter ratio (or after-body ratio) strongly influences the drag coefficient, producing first a maximum and then a minimum as the ratio increases.

4. For discs and cylinders with their axis of symmetry normal to the direction of fall, the length-to-diameter ratio, or aspect ratio, has little influence in the range of from 10:1 to 1:1, but a minimum does occur at the latter ratio. When this ratio falls below 0.5, the drag coefficient rises rapidly.

5. For rectangular prisms, the aspect ratio and after-body ratio interact with each other to influence the drag coefficient. The after-body ratio produces a variation in drag coefficient similar in form to that for discs and cylinders in the face-on orientation. But, the values of after-body ratio at which the maximum and minimum in the drag coefficient occur depend on the aspect ratio.

6. Analysis shows that the amplitude of a particle's oscillation in response to wake-shedding forces (as commonly observed in liquid media) is directly proportional to the fluid density. The response to wake-shedding, as manifested by oscillation, should be much less in a gas than in a liquid. It is also shown that the travel distance required to correct a non-stable orientation by fluid dynamic torque is inversely proportional to the square root of the fluid density. A particle may travel in a non-stable orientation much farther in a gas than in a liquid.

7. We have proceeded from the point of view that the range of N_{Re} selected in this study is the one most commonly encountered in actual solids/gas operations. Since in practically all such cases the particles are either accelerating or decelerating, the results presented here should find wide applicability for simulation, design, or optimization purposes. Data for nonspherical particles should also find use as first approximations for such irregular shapes as particles of coal, wood waste, industrial dusts and crushed mineral ores.

In view of the complexity of the fluid-mechanical phenomena associated with particle motion in this N_{Re} range (especially those accompanying wake-shedding) and of the considerable experimental difficulties in estimating their separate and coupled effects, we felt that an analytical solution is beyond the current state of knowledge. The only practical approach currently available is to correct for departure from ideal, constant-velocity conditions by means of an appropriate value of the drag coefficient.

Particulate motion has been under study in these laboratories for over two decades. A fairly comprehensive review of the literature up to about 1960 was presented in a series of articles by Torobin and Gauvin (1959-1961). This was updated by Clift and Gauvin (1971)* and more recently by Clift, Grace and Weber (1978). Only those works which are most pertinent to the topic of the present study will be reviewed here.

ACCELERATION AND DECELERATION

Unsteady relative velocity between a particle and a surrounding fluid is classified as acceleration if it is increasing and deceleration if it is decreasing, regardless of the change in the velocity of the particle relative to fixed coordinates in spaces.

Under steady-state conditions of constant relative velocity between a smooth, non-rotating sphere in rectilinear motion through an undisturbed, unbounded fluid, the drag force F_D on the particle is expressed in terms of the coefficient of drag C_D by means of the following correlation:

$$F_D = C_D A_p \rho U^2/2 \qquad (1)$$

Based on experimental and analytical results, the values of C_D and their dependence on the Reynolds number are best expressed analytically by the three equations of Beard and Pruppacher (1969) up to N_{Re} of 200 and by the expression proposed by Clift and Gauvin (1971) for the transitional and Newton regimes ($N_{Re} < 10^5$):

$$C_D = (24/N_{Re})(1 + 0.15\, N_{Re}^{0.687}) + 0.42/(1 + 4.25 \times 10^4\, N_{Re}^{-1.16}) \qquad (2)$$

It is important to note that both sets of analytical expressions give values of C_D which fall very close to those represented by the Standard Drag Coefficient Curve (e.g., Bailey 1974, and Clift et al. 1978). For practical purposes, therefore, the latter will be used as the standard of comparison.

For unsteady motion (acceleration or deceleration), two approaches have been proposed to predict the motion of the particle. The first assumes the value of the instantaneous coefficient of drag to equal the coefficient of drag for steady motion (as given above) at a velocity equal to the instantaneous relative velocity. This has the advantage of considerable simplicity, but in many situations has been proven to be seriously inaccurate. It becomes a valuable method to the extent that acceleration-dependent correction factors become available, primarily through experiment. This is the approach which has been followed in the present study.

The second approach is based on a generalization of Basset's equation by Odar and Hamilton (1964) and by Odar (1966), yielding the following expression for the instantaneous drag on a sphere:

$$F_D = C_D A_p \rho U^2/2 + C_A \rho v (dU/dt) + C_H D^2 \rho (\pi\nu)^{1/2} \int_0^t \frac{dU}{dz} \times \frac{dz}{\sqrt{t-z}} \qquad (3)$$

In this expression, the first term on the right of Equation (3) is the steady drag, with C_D taking on its value for steady motion for the same N_{Re}. The second term represents the "added mass" of fluid accelerated with the particle, while the third represents the dependence of drag on the conditions leading up to the present instant and contains the "Basset history integral." The last two terms on the right account for the effects of unsteady motion on the drag force. Any external potential forces (gravitational, electric, magnetic, etc.) must be added to the right hand side of the equation.

Strictly, Equation (3) should apply to creeping flow only, but Odar (1966) claims that it can be extended to much higher values of N_{Re} by means of the empirical coefficients C_A and C_H.

Considering first the added-mass effect, which arises from the inertia of the fluid entrained in the flow fluid of the particle, it can be said that the mass of the fluid entrained by the sphere (which is at most half of the volume of the sphere) is negligibly small compared to the mass of the sphere, when the fluid is a gas.

Regarding the Basset history term, it applies principally to a particle starting from rest and arises from the extra momentum transfer required to entrain fluid into the flow field around the particle. Very high values of the apparent drag coefficient are measured for the initial motion. This effect is generally considered to be over when the particle has travelled a distance equal to ten times its own diameter (see most recently Deffenbaugh and Marshall, 1976, or Coutanceau and Bouard, 1977). In the present experiments this condition was always satisfied. A term of this form may also occur when the Reynolds number of the particle changes rapidly with distance, and the flow pattern around the particle lags in its adjustment. This was the situation encountered by Lewis and Gauvin (1973) in their study of the motion of particles in a plasma jet. In this study, characterized by low relative N_{Re} (0.2 to 20) and extremely high deceleration rates (up to -2000 g), C_D increased over the standard curve values; this was correlated by means of the Basset term. In the present investigation, N_{Re} changed little over the test distance.

To summarize the situation, it can be concluded that the absence of added-mass and history effects is common to most practical cases of particle motion in gases. Nonetheless, deviations from the standard C_D-vs-N_{Re} curve have been found in some studies. Lunnon (1924), Buzzard and Nedderman (1967), and Mockros and Lai (1969) have measured the drag on spheres accelerating under gravity in nominally still air. In the Reynolds number range 2,000 to 50,000 and at accelerations up to 8 m/s^2, Lunnon found the drag coefficient to rise in an orderly manner with acceleration. However, our detained analysis of Lunnon's data indicated that it is highly likely that turbulence, and not acceleration effects, was responsible for his findings. Buzzard and Nedderman found no effect of acceleration at Reynolds numbers between 1,000 and 3,000. The works of Mockros and Lai (1969) and of Lai (1974) are often quoted as proof of the existence of added-mass and history effects. These authors did not report their data in the form of drag coefficient values, but in fact, a careful analysis of their experimental data indicates that the standard drag coefficient curve gives a reasonable fit to their particle time-distance histories.

Charters and Thomas (1945), Goin and Lawrence (1968) and Bailey and Hiatt (1972) injected spheres into still air and observed the drag coefficient under deceleration. None of these studies showed the unsteady velocity to produce any significant deviation from the standard curve, for Reynolds numbers from 200 to 100,000 and decelerations up to 120 m/s^2.

A third class of experiment explored the entrainment of particles by a moving steam of gas. Crowe (1962),

* This paper presents a few preliminary data on shape effects taken from the present study.

Rudinger (1970), Selberg and Nicholls (1968) and Schuyler (1969) all found deceleration in this situation to produce drag coefficients above the standard curve. Wang (1969) also observed increases in C_D during the entrainment of spheres and was able to correlate the results jointly with deceleration and free-stream fluid turbulence.

Ingebo (1956) appears to be the only worker to have reported a drag coefficient decrease during entrainment. However, Arrowsmith and Foster (1973) have suggested that this decrease was only apparent—that in fact, the fluid velocity was reduced by momentum transfer to the particles so that the relative velocity was less than that assumed by Ingebo. In summary, the magnitude, the direction, and even the existence of an effect of unsteady velocity on drag coefficients in gaseous media remains uncertain in the light of previous studies.

PARTICLE SHAPE

Of the numerous studies of the effect of shape on the drag of freely-moving particles, by far the greater number have been done in liquid media. In liquids, in the Reynolds number range of the present study (10^3 to 10^4), particles are commonly observed to respond to wake-shedding forces by oscillating or rotating. It would be useful at this time to examine the magnitude of this response when the fluid is a gas.

Interaction between a fluid and a particle in motion relative to each other comprises three components: a drag force acting in the mean direction of the relative motion, a lift force acting perpendicular to this direction, and a twisting moment or torque tending to re-orient the particle. For simplicity, the moment is assumed to act about an axis normal to the direction of travel. Thus, the lift force and the torque can be represented by

$$L = C_L A_p \rho U^2/2 \tag{4}$$

$$T = C_T A_p \rho U^2 D/2 \tag{5}$$

1. Considering first the response of a particle to wake-shedding, the instantaneous lift and torque are both seen to be period functions of time. For simplicity, it is assumed that

$$C_L = C_{Lm} \sin(2\pi f\theta) \tag{6}$$

$$C_T = C_{Tm} \sin(2\pi f\theta) \tag{7}$$

where f is the wake-shedding frequency, given by $f = N_{St}U/D$. Then the lateral and rotational equations of motion are

$$Md^2h/d\theta^2 = C_{Lm}A_p\rho U^2 \sin(2\pi f\theta)/2 \tag{8}$$

and

$$Id^2\alpha/d\theta^2 = C_{Tm}A_p\rho U^2 D \sin(2\pi f\theta)/2 \tag{9}$$

which can be integrated to give

$$h = -C_{Lm}[A_p\rho U^2/M(2\pi f)^2]\sin(2\pi f\theta)/2 \tag{10}$$

and

$$\alpha = -C_{Tm}[A_p\rho U^2 D/I(2\pi f)^2]\sin(2\pi f\theta)/2 \tag{11}$$

Thus, for a given particle, the amplitude of the two oscillatory motions is directly proportional to the fluid density.

2. If for any cause the particle finds itself in an orientation where the steady fluid dynamic torque is not zero, then the subsequent angular motion is described by

$$Id^2\alpha/d\theta^2 = C_T A_p \rho U^2 D/2 \tag{12}$$

In general, C_T is a function of α, but ignoring this dependence and integrating twice (assuming $d\alpha/d\theta = 0$ at time zero) gives

$$\Delta\alpha = C_T A_p \rho U^2 D(\Delta\theta)^2/2I = C_T A_p \rho D(\Delta s)^2/2I \tag{13}$$

That is, for a given particle, the distance, Δs, required to produce a change of $\Delta\alpha$ in the orientation angle α is inversely proportional to the square root of fluid density ρ. *Thus a particle is able to travel much farther in an unstable orientation in a gas than it can in a liquid.*

3. If the orientation angle α is changing with time, the instantaneous values of C_D, C_L and C_T are bound to exhibit some dependence on the rate of change, $(d\alpha/d\theta)$. Kry and List (1974) have shown mathematically that for a particle rotating at frequency f', the effect of non-steady orientation can be ignored if

$$N'_{St} = f'D/U < 0.04 \tag{14}$$

That is, for values of N'_{St} below 0.04, the motion is quasi-steady and the particle can be considered as passing through a succession of fixed orientations. The frequency f' is related to $(d\alpha/d\theta)$ by

$$f' = (d\alpha/d\theta)/(2\pi) \tag{15}$$

so that Kry and List's criterion becomes

$$(d\alpha/d\theta)(D/U) < 0.08\pi \tag{16}$$

Considering the change in angle $\Delta\alpha$ calculated by Equation (13), the angular velocity at the end of that change is shown by integrating Equation (12) once to be

$$d\alpha/d\theta = C_T A_p \rho U D \Delta s/2I \tag{17}$$

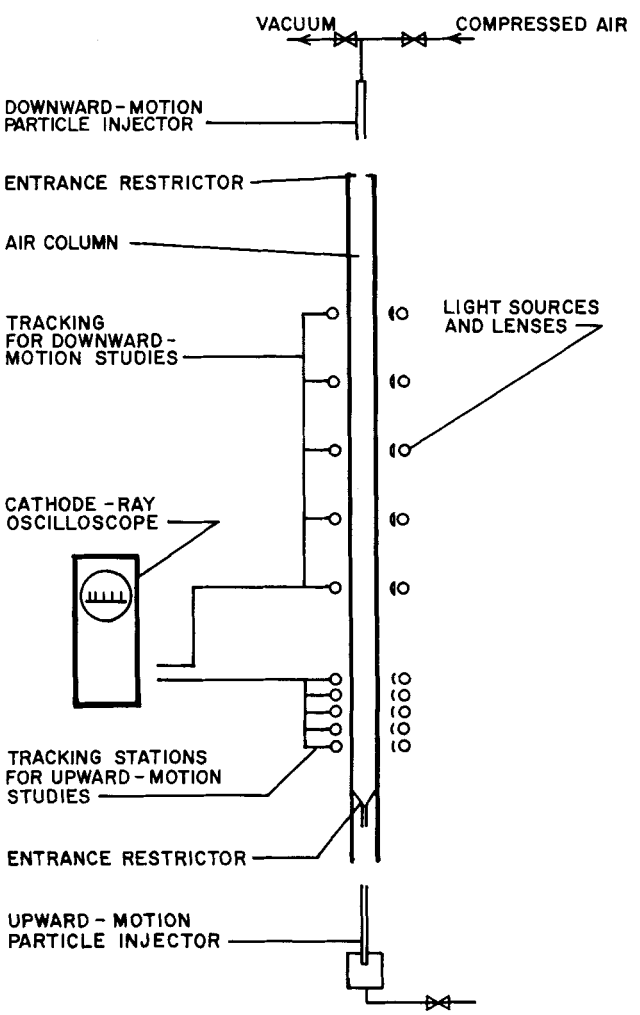

Figure 1. Arrangement of test apparatus.

TABLE 1. SPHERES TESTED IN DOWNWARD MOTION

Particle No.	Material	Density, g/cm³	Diameter, cm
1	Acrylic	1.19	0.2962
2	Acrylic	1.19	0.4953
3	Acrylic	1.19	0.7978
4	Aluminum	2.70	0.4762
5	Aluminum	2.70	0.7938
6	Steel	7.80	0.2381
7	Steel	7.80	0.3969
8	Tungsten carbide	14.90	0.1588
9	Tungsten carbide	14.90	0.3125

Substituting for Δs from Equation (13) and inserting into the inequality (16) gives:

$$(C_T A_p \rho D^3 \Delta\alpha / 2I)^{1/2}/\pi < 0.08 \qquad (18)$$

For a given change in orientation, the Kry and List rate-of-change criterion is proportional to the square root of fluid density. *Hence, motion in a gas has a greater probability of being quasi-steady than motion in a liquid.*

This analysis shows that the average drage force on a rotating particle in a gas may be estimated as the average of what the drag forces would be if the particle were fixed in each of the orientations through which it passes. This approach is analogous to that taken by Pasternak and Gauvin (1961) who used an averaging technique to estimate the rate of heat and mass transfer to accelerating, freely-rotating cubes and cylinders in a turbulent hot air stream. The present study provides such fixed-orientation data by studying freely-moving but non-rotating particles. These data are compared with those from fixed-body tests. They are also compared with the results of some of the few other free-motion studies that have been made in gases, particularly the studies of Eiffel (1907) and by Christiansen and Barker (1965).

EXPERIMENTAL

All experiments were carried out in still air in a vertical column 6.1 m high by 0.203 m in diameter. Particle dimensions ranged from 0.25 to 2.54 cm and particle density from 0.074 to 14.9 g/cm³. Particle injectors, driven by compressed air, were located outside the top and bottom of the column. In each test, a particle was impelled up or down along the centreline of the column, and its time-distance history was determined using a photoelectric-cell tracking system. Data were analyzed to determine velocity, acceleration, and a mean drag coefficient value. A schematic view of the equipment is shown in Figure 1.

TABLE 2. NON-SPHERICAL PARTICLES TESTED IN DOWNWARD MOTION

Cylinders and discs

Ident. No.	Orientation	Diam. D, cm	Length L, cm	L/D	Mass M, grams	Material
503	Axis horizontal	0.945	0.263	0.278	0.3430	Composite
510	Axis horizontal	0.953	0.490	0.515	0.6023	Composite
102	Axis horizontal	0.315	0.323	1.024	0.0723	Aluminum
213	Axis horizontal	0.318	0.566	1.79	0.1215	Aluminum
211	Axis horizontal	0.236	0.642	2.72	0.0771	Aluminum
238	Axis horizontal	0.173	0.617	3.57	0.1146	Copper
234	Axis horizontal	0.140	0.640	5.04	0.0870	Copper
325	Axis horizontal	0.099	0.655	6.61	0.04085	Steel
251	Axis horizontal	0.077	0.626	8.16	0.03465	Gold
229	Axis horizontal	0.062	0.640	10.24	0.01836	Copper
501	Axis vertical	0.645	2.692	4.17	0.6480	Composite
500	Axis vertical	0.645	1.267	1.97	0.4740	Composite
511	Axis vertical	0.643	0.770	1.20	0.5770	Composite
113	Axis vertical	0.965	0.767	0.794	0.3234	Wood
100	Axis vertical	0.634	0.376	0.593	0.3202	Aluminum
104	Axis vertical	0.630	0.185	0.294	0.5147	Copper
101	Axis vertical	0.635	0.160	0.251	0.1359	Aluminum
107	Axis vertical	0.658	0.155	0.235	0.3908	Steel
108	Axis vertical	0.630	0.074	0.117	0.1883	Steel

Rectangular prisms

Ident. No.	Dimensions A, cm	B, cm	C, cm	Aspect ratio, A/B	Afterbody ratio, C/B	Mass M, grams	Material
427	0.620	0.620	0.080	1.000	0.1282	0.2387	Steel
413	0.625	0.622	0.156	1.000	0.251	0.4818	Steel
416	0.571	0.571	0.292	1.000	0.511	0.1055	Celite
415	0.576	0.576	0.574	1.000	0.995	0.1867	Celite
512	0.625	0.625	0.612	1.000	0.980	0.5080	Composite
504	0.320	0.315	0.737	1.015	2.34	0.1390	Composite
505	0.318	0.318	1.217	1.000	3.73	0.2730	Composite
437	0.635	0.315	0.081	2.020	0.256	0.1270	Steel
436	0.635	0.318	0.160	2.000	0.504	0.2579	Steel
419	0.572	0.302	0.302	1.890	1.000	0.0567	Celite
506	0.620	0.318	0.632	1.950	1.993	0.5190	Composite
429	0.632	0.158	0.158	4.000	1.000	0.1251	Steel
508	1.270	0.330	0.671	3.850	2.03	0.3690	Composite

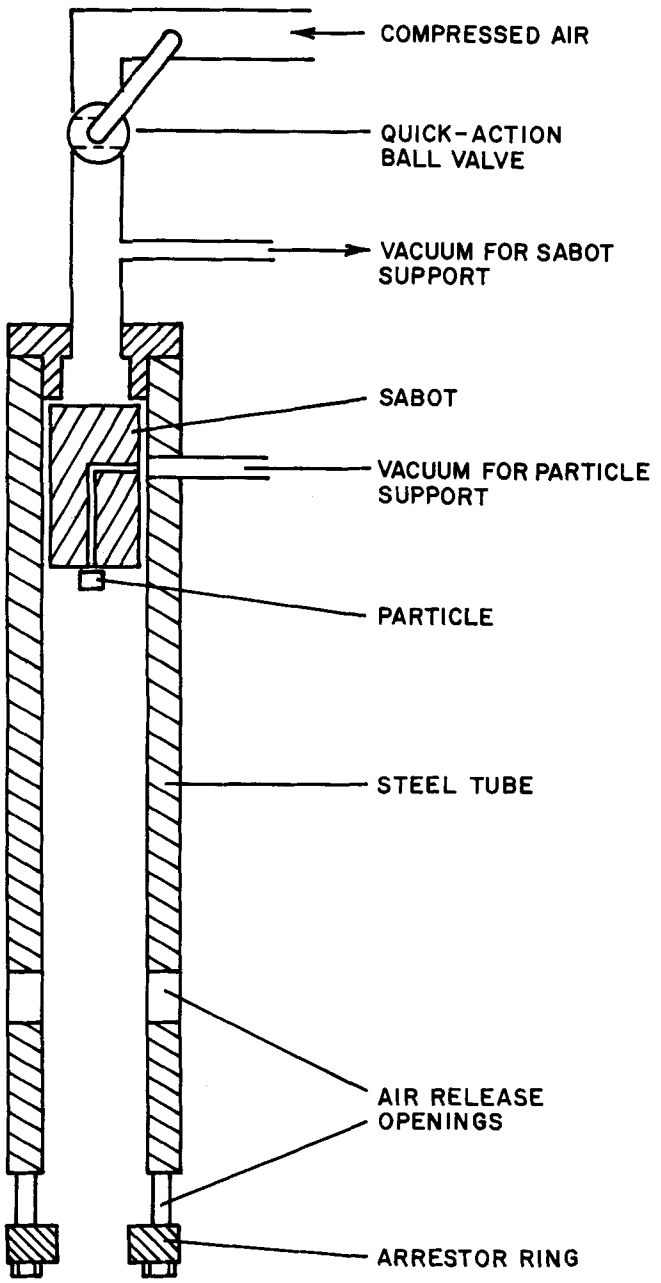

Figure 2. Particle downward injector.

Particles

Great care was exercised in the selection and/or preparation of the test particles. Selberg and Nicholls (1968) have ascribed the increase in C_D over the standard curve in their study of small spheres accelerating in a laminar air flow to the rough surface of their spheres.

Four classes of particles were used in the study:

1. Seventeen light-weight pith and celite spheres for upward-motion deceleration studies, with diameters from 0.196 to 1.27 cm and specific gravity from 0.074 to 0.98.
2. Nine commercially-made spheres, described in Table 1, for downward-motion acceleration studies.
3. Twenty-two homogenous discs, cylinders and rectangular prisms, described in Table 2, for downward-motion terminal-velocity studies.
4. Ten composite discs, cylinders and rectangular prisms, described in Table 2, for downward-motion terminal-velocity studies in non-preferred orientations.

Two of the homogeneous discs (No. 101 and 107) listed in Table 2 were also subjected to downward-motion acceleration study.

The non-spherical particles all required careful construction. All surfaces were aerodynamically smooth, edges were sharp, and the distance between nominally parallel faces was constant to within 0.0025 cm. The non-homogeneous particles were eccentrically weighted to shift the center of gravity below the center of hydrodynamic pressure in the orientation we desired to study. For prismatic shapes, two existing particles, one made of steel or copper and the other of balsa wood, were glued together. For cylinders and discs, a partially hollow construction was used.

Particle Injectors

In both the upward and downward-motion tests, the particle was given an initial velocity by injection, using a vertical metal tube with a circular sabot inside, free to traverse the length of the tube. The particle rested on top of the sabot in the upwards studies and was held by vacuum against the bottom of it until the moment of injection in the downwards studies. The sabot was impelled by compressed air at various pressures to vary the injection velocity. Motion of the sabot was arrested by a ring at the exit of the tube, but the particle continued on into the test column.

The downward injection device (see Figure 2) required considerable development effort. Vacuum had to be provided to support both the sabot and the particle prior to firing.

An injector used in the downward-motion tests achieve terminal velocity without the need for a long fall path, such as would have been required if the particle had started from rest.

Particle Tracking System

The time-distance history of the particle in each test was measured by photoelectric cells connected to an oscilloscope, as shown in Figure 1. Light beams were focused using a system of crossed cylindrical lenses. Each beam was concentrated at the centerline of the column into a strip about 1.9 cm in horizontal width and of negligible vertical thickness, thus localizing and intensifying the electrical signal. Spheres as small as 0.08 cm in diameter were tracked successfully with this system.

Data Analysis

Treatment of the data for each test rested on the assumption of a constant drag coefficient, C_D, over the tracking zone. The procedure was to assume various values for the particle velocity U_1 at the first station, and for the drag coefficient. The equation of motion was then integrated to predict a time-distance history. A nested "golden section" search routine was used to determine the combination of U_1 and C_D which produced the minimum sum of the squares of the deviations of predicted times from measured times at the other four tracking stations. Using the methods described by Draper and Smith (1968) for non-linear least squares, the confidence limits for the C_D estimates were also calculated.

In the case of the upward-motion (deceleration) and the downward acceleration tests, a value of C_D was produced, and, at the middle tracking station, a value of acceleration or deceleration, and of Reynolds number. The rest of the downward-motion tests were performed close to terminal velocity and were intended to show the effect of particle shape on drag coefficient. Several tests were performed on each particle, and results were combined to obtain a single value for C_D. This value was calculated by arithmetical averaging of the individual test values, after first weighting them inversely according to the square of the confidence limit for the individual test. The greatest reliance was put on those tests which had produced the most clear-cut results. The confidence limit for this average was obtained from the deviations of the individual values about the average, after applying a similar weighting, as above, to accentuate the best established results.

RESULTS AND DISCUSSION

The experiments fall into three groups, namely, deceleration tests on light spheres, acceleration tests on spheres and discs, and constant-velocity tests on particles of various shapes. The results for each group follow.

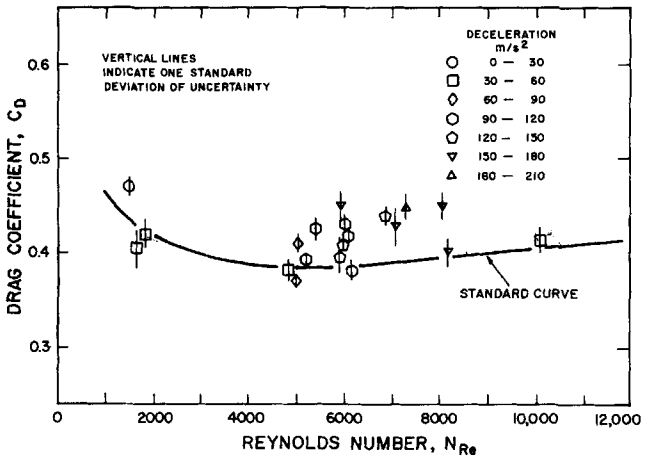

Figure 3a. Deceleration drag data for upward-moving spheres.

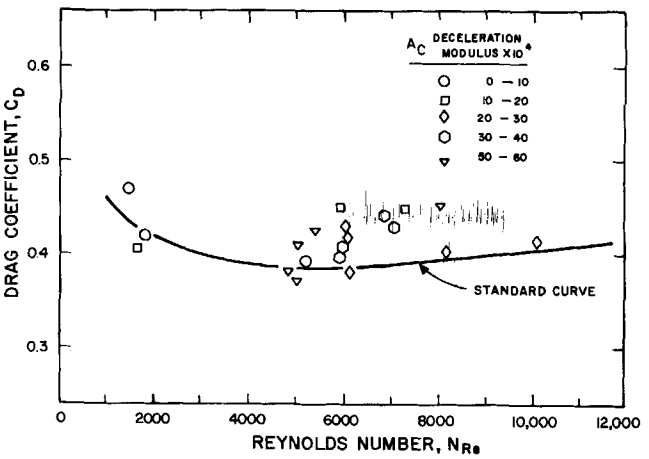

Figure 3b. Deceleration drag data for upward-moving spheres.

Decelerating Spheres

Figures 3a and 3b show the data for light spheres moving upwards and decelerating at rates up to 210 m/s². The data points are identified in one plot according to the magnitude of their deceleration, and in the other, according to the value of their deceleration modulus, A_c, defined as $|\dot{U}|D/U^2$. In Figure 3a, the vertical line through each point shows the standard deviation of the uncertainty interval. Taken together, the drag coefficients fall a small but significant amount (about 10%) above the standard curve. They thus agree, at least qualitatively, with Crowe (1962), Rudinger (1970), Selberg and Nicholls (1968) and Schyler (1969). The results of these earlier works have been suggested in the literature as due variously to inter-particle interference, surface roughness, and particle deformation. The present results are free from such influences and therefore add significant new evidence to the opinion that deceleration can increase the drag coefficients of spheres. By contrast, Charters and Thomas (1945), Goin and Lawrence (1968) and Bailey and Hiatt (1972) observed no such effect.

One difference between the studies in which C_D rose and those in which it did not is in the range of the values of the deceleration modulus. In the present study it ranged from 6×10^{-4} to 6×10^{-3}; in Crowe's work the range was 2×10^{-3} to 5×10^{-3}. If the deceleration is induced primarily by fluid dynamic drag, then it is readily shown that the deceleration modulus is inversely proportional to particle density.

In the other studies where an increase in C_D was observed, the particle densities were similar to those presented here. The deceleration modulus probably lay in the same range, as is the case for instance in Crowe's work. In the studies where no effect was observed, the values of the modulus were about an order of magnitude lower. In the case of Charters and Thomas and of Goin and

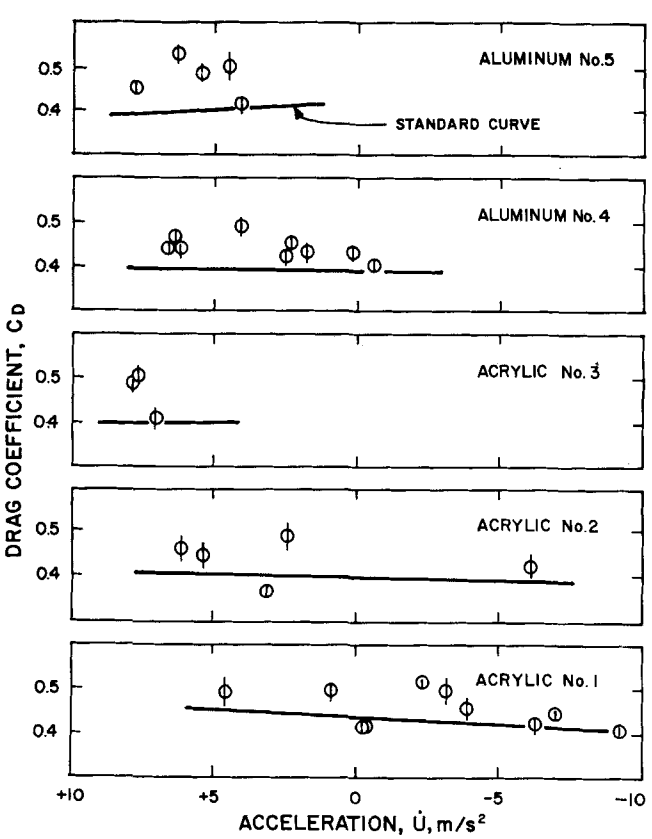

Figure 4a. Acceleration drag data for downward-moving spheres.

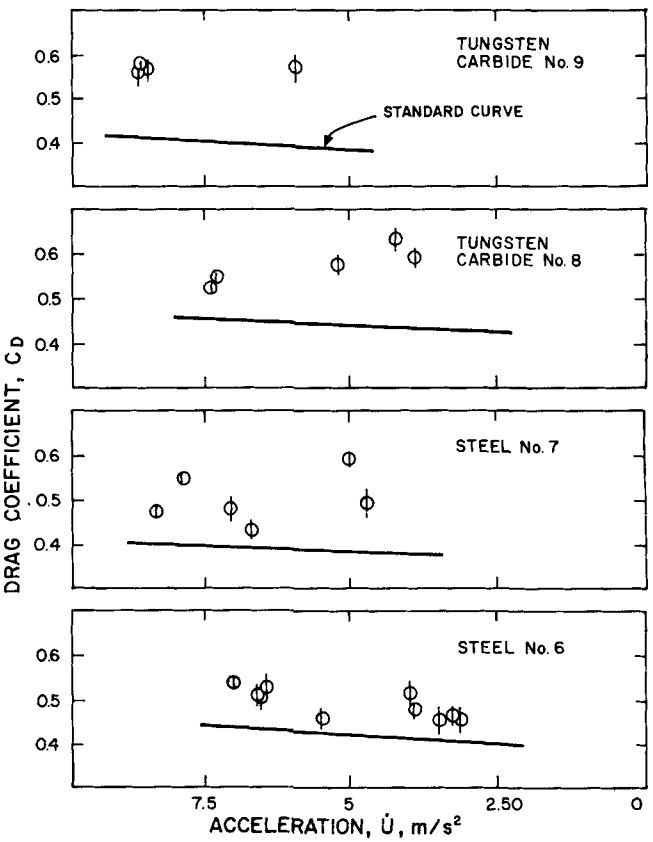

Figure 4b. Acceleration drag data for downward-moving spheres.

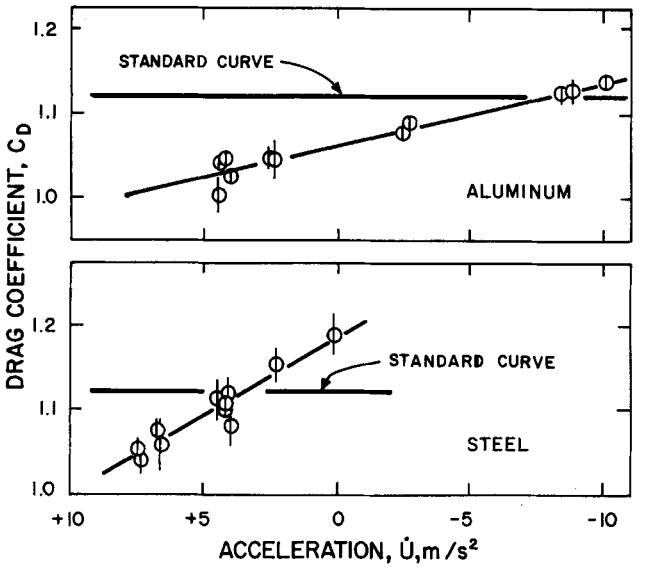

Figure 5a. Acceleration drag data for downward-moving discs.

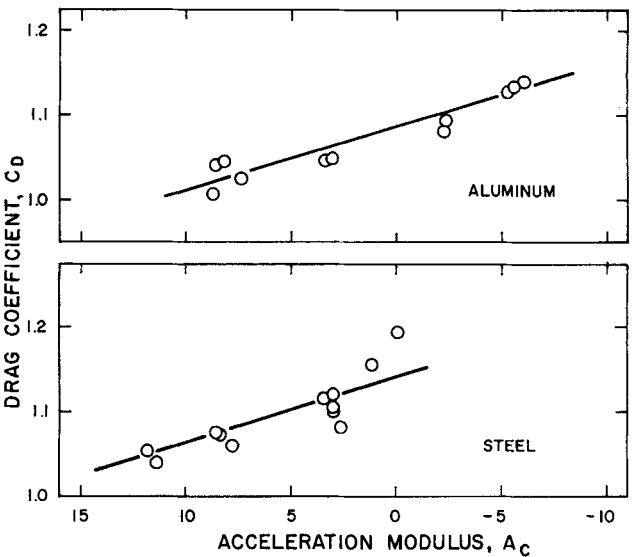

Figure 5b. Acceleration drag data for downward-moving discs.

Lawrence, the low modulus resulted from the high density of their spheres. Bailey and Hiatt used spheres of both high and low density, but careful consideration of their experimental conditions indicates that the deceleration modulus never exceeded 5.5×10^{-5}. The deceleration modulus is a measure of the inability of the flow field around the particle to adjust to changing relative velocity; it thus has fundamental significance.

A possible explanation for the increase in drag coefficient is that the boundary-layer separation circle is pushed forward. Mager (1969) has shown experimentally that deceleration can produce inflection in the boundary-layer velocity profile, which could lead to premature separation. Yoshizawa (1975) has demonstrated mathematically that the separation circle can shift forward during deceleration.

Accelerating Spheres and Discs

Figure 4a shows the data for acrylic and aluminum spheres, Figure 4b for steel and tungsten carbide spheres. The level of uncertainty is shown by the vertical lines; the prediction of the standard drag coefficient curve for the corresponding Reynolds numbers is shown by the solid, approximately horizontal, line. Data indicate no apparent effect of acceleration, but rather a tendency for drag coefficient to increase with particle density.

Results for acrylic spheres lie close to the standard curve. This finding agrees with that of Buzzard and Nedderman (1967) for nylon spheres of similar density and also with those of Mockros and Lai (1969), who worked with spheres of specific gravity 0.03 to 0.6. These results also prove the validity of the experimental procedure and of the data analysis used here—the present study is unique in its combination of high-density spheres and still air.

The ratio of particle density to fluid density is well known as a factor affecting the drag coefficient in liquid media (see, for instance, Isaacs and Thodos 1967). The sense of the effect is, however, opposite to the present findings. Blizard (1924) derived the following equation from measurements in a gaseous medium

$$C_D = 5.7(\rho_p/\rho)^{0.308} N_{Re}^{-0.428} \qquad (19)$$

which is in the same sense as the present finding. However, the Reynolds number dependency indicates that the equation is restricted to a range lower than that of the present study. A density effect implies the presence of some rotational or oscillatory type of particle secondary motion. This motion depends on the ratio of particle-to-fluid density and affects drag by altering the flow patterns around the particle. It was shown earlier that the amplitude of such motion decreases as the ratio of particle-to-fluid density increases, so apparently, some small amount of secondary motion actually decreases the drag coefficient. Measurements on fixed spheres would be valuable for comparison. Such data appear unavailable in the Reynolds number range 10^3 to 10^4: the standard C_D vs. N_{Re} curve in that range is based on Lunnon's (1928) free-fall tests in water and on Wieselsberger's (1922) wind-tunnel tests in which the sphere was supported as a moveable pendulum.

Data for accelerating discs are shown in Figures 5a and 5b. Three observations emerge: (1) at all accelerations including zero there is an effect of particle density on drag, (2) the drag coefficient decreases as acceleration increases, and (3) comparing the two discs, the rates of drag reduction with acceleration modulus are more nearly the same than are the rates with acceleration alone.

The density effect is in the same sense as for spheres and amounts to about 5% difference between the steel and aluminum discs at the same value of the acceleration modulus. Two possible explanations for the acceleration effect were examined but rejected. First, we noted the Reynolds numbers of the test points; the data were compared with the C_D -vs.-N_{Re} experimental curve of Roos and Willmarth (1971). C_D variations found in the present tests were in the same direction, but of much greater magnitude. Second, the expression derived by Mavis (1970) in his experimental study of the added mass of discs in the face-on orientation was evaluated for the two discs. Not only was the prediction of Mavis an order of magnitude lower than the effect observed here, but it was in the opposite direction. The true reason for the observed effect probably requires a detailed analysis of the time-dependent equations of fluid motion around a bluff body. That the acceleration modulus, rather than the acceleration, is the correlating parameter might serve as a guide in such an analysis.

Particles at Constant Velocity

A summary of the averaged results for the thirty-two nonspherical particles tested under conditions of approxi-

TABLE 3. CONSTANT-VELOCITY DRAG COEFFICIENTS FOR DOWNWARD-MOVING NON-SPHERICAL PARTICLES

Discs & cylinders, axis horizontal		Discs & cylinders, axis vertical		Rectangular prisms	
Ident. No.	Drag coeff.	Ident. No.	Drag coeff.	Ident. No.	Drag coeff.
503	1.16	501	0.92	427	1.14
510	0.70	500	0.87	413	1.22
102	0.75	511	0.71	416	1.04
213	0.67	113	0.96	415	1.02
211	0.66	100	1.11	512	1.08
238	0.72	104	1.18	504	1.06
234	0.72	101	1.06	505	1.06
325	0.75	107	1.19	437	1.07
251	0.80	108	1.15	436	1.25
229	0.81			419	0.925
				506	1.06
				429	1.23
				508	1.10

mately constant velocity is given in Table 3. The tests were conducted before the particle density effect was observed in the acceleration tests. Consequently, the materials of particle construction were chosen solely on the basis of convenience. We considered the magnitude of the density effect in the constant-velocity tests sufficiently small to allow valid conclusions with regard to shape effects to be drawn from the data.

Three combinations of shape and orientation were tested: cylinders and discs with axis horizontal (i.e., normal to the direction of travel), cylinders and discs with axis vertical, and rectangular prisms with various faces normal to the direction of travel. Data are discussed for each of these combinations.

Cylinders and Discs with Axis Horizontal. The drag coefficients are shown as a function of the ratio of particle diameter to axis length in Figure 6. For ratios less than 1.0, data are seen to be in reasonable agreement with those of previous works. No previous data appear to exist for ratios greater than 1.0. Tests at these higher ratios required eccentrically weighted particles to achieve the desired orientation. At D/L of 2, the behavior is similar to that of cylinders, but by 3.5, the nature of the flow field around the particle appears to change, producing a higher drag coefficient.

Cylinders and Discs with Axis Vertical. The drag coefficients are plotted in Figure 7 against the after-body ratio, which for these particles is the ratio of length or thickness to diameter. Data for L/D ratios greater than 1.0 were obtained with eccentrically-weighted particles. Also shown is the curve presented by Hoerner (1958),

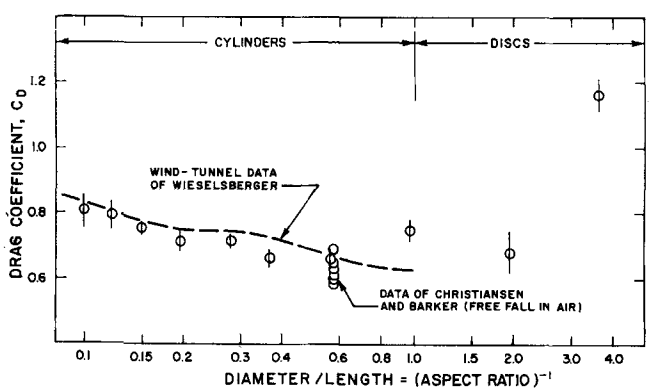

Figure 6. Constant-velocity drag for cylinders and discs with axis normal to direction of travel.

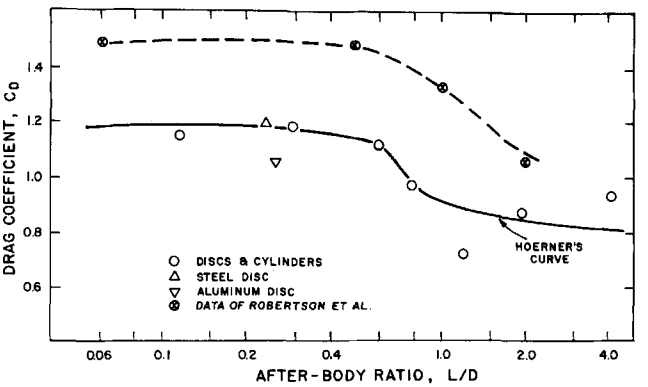

Figure 7. Constant-velocity drag for cylinders and discs with axis parallel to direction of travel.

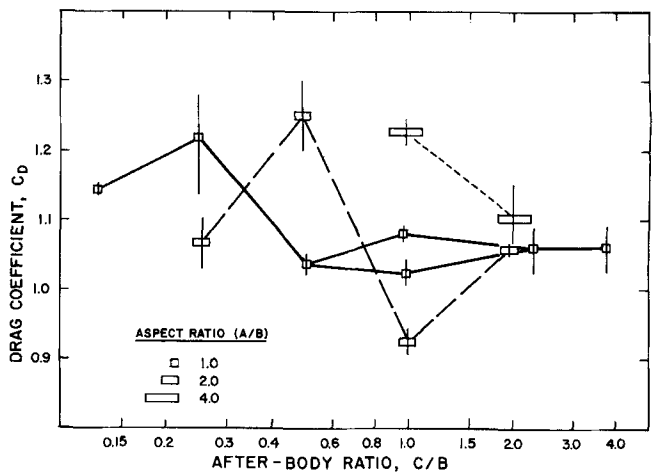

Figure 8. Constant-velocity drag for rectangular prisms in face-on orientations.

which is based largely on the work of Eiffel (1907), and the recent data of Robertson et al. (1972). Although the latter results are considerably higher than those of Eiffel or of the present study, all three data sets indicate a change in flow pattern in the vicinity of L/D equal to 1.0. A study by Calvert (1967) shows that when L/D reaches approximately this value, the flow which separates at the leading edge can re-attach to the sides of the cylinder. A higher base pressure results and the drag coefficient decreases. As seen in the present study, if L/D increases beyond 1.0, a steady increase in drag may be

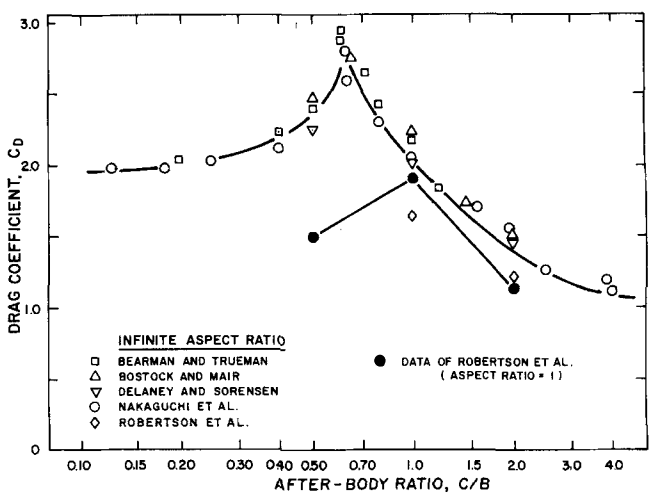

Figure 9. Drag on rectangular prisms of finite and infinite aspect ratios.

expected, because of friction on the side of cylinder. The discrepancy with Robertson's data is not explained.

Rectangular Prisms with a Face Normal to the Direction of Travel. The drag coefficients are shown in Figure 8 as a function of two parameters: the aspect ratio which describes the cross-section normal to the direction of travel and is the ratio of the longer (A) to the shorter dimension (B), and the after-body ratio, which is the ratio of dimension (C) in the direction of travel to dimension (B). For the prisms of aspect ratio 1.0, the behavior is similar to that of the circular cylinders shown in Figure 7. Reattachment appears complete by the time C/B reaches a value of 0.5, but the decrease in drag coefficient is not as great as for circular cylinders. Particles with an aspect ratio greater than 1.0 also characteristically decrease in drag coefficient, but a higher value of C/B is required.

For the aspect ratios of 1.0 and 2.0, there occurs a maximum C_D. This has been observed by others in tests on fixed prisms spanning a wind tunnel, where the aspect ratio A/B is considered to be infinity. Data of Nakaguchi, Hashimoto and Muto (1968), of Bostock and Mair (1972), of Bearman and Trueman (1972), of Delaney and Sorensen (1959) and of Robertson et al. (1972) are shown in Figure 9. The same general pattern is followed in all cases.

The explanation for the maximum in C_D at C/B of around 2/3 is suggested by the wake studies of Fail, Lawford and Eyre (1959) and of Calvert (1967). Measuring the pressure in the wake of thin plates normal to flow, the point of minimum pressure lay, not at the rear surface, but some distance downstream. The rear surface of a plate of greater thickness intrudes into this region of minimum pressure and causes the plate to experience a higher drag force. This explanation ignores the influence that plate thickness must have on the form of the wake.

As a general conclusion to this study, we can say that, in view of the complexity of the fluid-mechanical phenomena associated with particle motion in this N_{Re} range, especially those accompanying wake-shedding, and in view of the considerable experimental difficulties in estimating their separate and coupled effects, it is probable that an analytical solution is beyond the current stage of knowledge. The only practical approach available now is to correct for departure from ideal, constant-velocity conditions with an appropriate value of drag coefficient, as experimentally derived in this study.

NOTATION

A = longer dimension of a particle in the plane normal to the direction of travel
A_p = projected area of a particle in the direction of travel
A_c = acceleration (or deceleration) modulus, $|\dot{U}|D/U/U$
B = shorter dimension of a particle in the plane normal to the direction of travel
C = dimension of a particle in the direction of travel
C_A = added mass coefficient
C_D = drag coefficient, $R/(\frac{1}{2}A_p\rho U^2)$
C_H = Basset's history coefficient
C_L = lift coefficient, $L/(\frac{1}{2}A_p\rho U^2)$
C_T = torque coefficient, $T/(\frac{1}{2}A_p\rho U^2 D)$
C_{Lm} = amplitude of fluctuating lift coefficient
C_{Tm} = amplitude of fluctuating torque coefficient
D = diameter of sphere, disc or cylinder; linear dimension of particle
F_D = drag force on particle
f = frequency of wake-shedding
f' = frequency of particle rotation
h = lateral displacement of particle
I = moment of inertia of particle
L = axis length of cylinder or disc; lateral lift force on particle
L' = distance travelled by particle
M = particle mass
N_{Re} = particle Reynolds number DU/ν
N_{Rec} = critical Reynolds number
N_{Sr} = Strouhal number of wake-shedding, fD/U
N'_{Sr} = Pseudo-Strouhal number of rotation
s = distance travelled in direction of mean motion
t = time
T = fluid dynamic torque exerted on particle
U = relative velocity between fluid and particle
$\dot{U}$ = rate of change of relative velocity between fluid and particle
v = volume of particle
z = convolution time (for history integral)

Greek Letters

α = orientation angle of particle with respect to direction of mean motion
θ = time
ν = kinematic viscosity of fluid
ρ = density of fluid
ρ_p = density of particle

LITERATURE CITED

Arrowsmith, A., and P. J. Foster, "The Motion of a Stream of Mono-sized Liquid Drops in Air," *Chem. Eng. J.*, **5** (3), 243 (1973).

Bailey, A. B., and J. Hiatt, "Free-Flight Measurements of Sphere Drag at Subsonic, Transonic, Supersonic and Hypersonic Speeds for Continuum, Transition and Near-Free-Molecular Flow Conditions," *AIAA J.*, **10** (11), 1436 (1972).

Bailey, A. B., "Sphere Drag Coefficients for a Broad Range of Mach and Reynolds Numbers," *J. Fluid Mech.*, **65** (2), 401 (1974).

Bassett, A. B., "On the Motion of a Sphere in a Viscous Liquid," *Quart. J. Math.*, **41**, 369 (1910).

Beard, K. V., and H. R. Pruppacher, "A Determination of the Terminal Velocity and Drag of Small Water Drops by Means of a Wind Tunnel," *J. Atmos. Sci.*, **26**, 1966 (1969).

Bearman, P. W., and D. M. Trueman, "An Investigation of the Flow around Rectangular Cylinders," *Aeronautical Quart.*, **23** (3), 229 (1972).

Blizard, J., "The Motion of Coke and Coal Particles in Gases," *J. Franklin Inst.*, **197**, 199 (1924).

Bostock, B. R., and W. A. Mair, "Pressure Distributions and Forces on Rectangular and D-Shaped Cylinders," *Aeronautical Quart.*, **23**, 1 (1972).

Buzzard, J. L., and R. M. Nedderman, "The Drag Coefficients of Liquid Droplets Accelerating through Air," *Chem. Eng. Sci.*, **22**, 1577 (1967).

Calvert, J. R., "Experiments on the Low-Speed Flow Past Cones," *J. Fluid Mech.*, **27**, 273 (1967).

Charters, A. C., and R. N. Thomas, "The Aerodynamic Performance of Small Spheres from Subsonic to High Supersonic Velocities," *J. Aeronautical Sci.*, **12**, 468 (1945).

Christiansen, E. B., and D. H. Barker, "The Effect of Shape and Density on the Free Settling of Particles at High Reynolds Numbers," *AIChE J.*, **11**, 145 (1965).

Clift, R., J. R. Grace and M. E. Weber, *Bubbles, Drops and Particles*, Academic Press, New York (1978).

Clift, R., and W. H. Gauvin, "Motion of Entrained Particles in Gas Streams," *Can. J. Chem. Eng.*, **49**, 439 (1971).

Coutanceau, M., and R. Bouard, "Experimental Determination of the Main Features of the Viscous Flow in the Wake of a

Circular Cylinder in Uniform Translation. Part 2: Unsteady Flow," *J. Fluid Mech.*, 79 (2), 257 (1977).
Crowe, C. T., "Drag Coefficients of Inert, Burning or Evaporating Particles Accelerating in Gas Streams," Ph.D. Thesis, University of Michigan, Ann Arbor (1962).
Deffenbaugh, F. D., and F. J. Marshall, "Time Development of the Flow about an Impulsively Started Cylinder," *AIAA J.*, **14**, 908 (1976).
Delaney, N. K., and N. E. Sorensen, "Low-Speed Drag of Cylinders of Various Shapes," NACA Tech. Note 3038 (1959).
Draper, W. R., and H. Smith, *Applied Regression Analysis*, John Wiley & Sons, Inc., New York (1968).
Eiffel, G., "Recherches à la Tour Eiffel," Paris (1907).
Fail, R., J. A. Lawford, and R. C. W. Eyre, "Low-Speed Experiments on the Wake Characteristics of Flat Plates Normal to an Air Stream," Aeronaut. Res. Council (Gt. Brit.), R. and M. No. 3120 (1959).
Goin, K. L., and W. R. Lawrence, "Subsonic Drag of Spheres at Reynolds Numbers from 200 to 10,000," *AIAA J.*, **6**, 961 (1968).
Hoerner, S. F., *Fluid Dynamic Drag*, published by the author, New Jersey (1958).
Ingebo, R. D., "Drag Coefficient for Droplets and Solid Spheres in Clouds Accelerating in Air Streams," NACA Tech. Note 3762 (1956).
Isaacs, J. L., and G. Thodos, "The Free-Settling of Solid Cylindrical Particles in the Turbulent Regime," *Can. J. Chem. Eng.*, **45**, 150 (1967).
Kry, P. R., and R. List, "Aerodynamic Torques on Rotating Oblate Spheroids; Angular Motions of Freely Falling Spheroidal Hailstone Models," *Phys. Fluids*, **17** (6), 1087 and 1093 (1974).
Lai, R. S., "Drag on a Sphere Accelerating Rectilinearly in a Maxwell Fluid," *Int. J. Eng. Sci.*, **12**, 645 (1974).
Lewis, J. A., and W. H. Gauvin, "Motion of Particles Entrained in a Plasma Jet," *AIChE J.*, **19**, 982 (1973).
Lunnon, R. G., "The Resistance of Air to Falling Spheres," *Phil. Mag.*, **47**, 1973 (1924).
Lunnon, R. G., "Fluid Resistance to Moving Spheres," *Proc. Roy. Soc. (London)*, **118A**, 680 (1928).
Mager, A., "Sudden Acceleration of a Laminar Boundary Layer by a Moving Belt," *AIAA J.*, **7**, 2247 (1969).
Mavis, F. T., "Virtual Mass of Plates and Disks in Water," *Proc. ASCE*, **96** (HY 10), 1947 (1970).
Mockros, L. F., and R. V. S. Lai, "Validity of Stokes' Theory for Accelerating Spheres," *Proc. ASCE*, **95** (EM3), 629 (1969).
Nakaguchi, H., K. Hashimoto and S. Muto, "An Experimental Study on Aerodynamic Drag of Rectangular Cylinders," (in Japanese) *J. Japn. Soc. Aeronaut. Space Sci.*, **16**, 1 (1968).
Odar, F., and W. S. Hamilton, "Forces on a Sphere Accelerating in a Viscous Fluid," *J. Fluid Mech.*, **18**, 302 (1964).
Odar, F., "Verification of the Proposed Equation for Calculation of the Forces on a Sphere Accelerating in a Viscous Fluid," *J. Fluid Mech.*, **25**, 591 (1966).
Pasternak, I. S., and W. H. Gauvin, "Turbulent Convective Heat and Mass Transfer from Accelerating Particles," *AIChE J.*, **7**, 254 (1961).
Robertson, J. A., C. Y. Lin, G. S. Rutherford and M. D. Stine, "Turbulence Effects on Drag of Sharp-Edged Bodies," *Proc. ASCE*, **98** (HY7), 1187 (1972).
Roos, F. W., and W. W. Willmarth, "Some Experimental Results on Sphere and Disk Drag," *AIAA J.*, **9**, 285 (1971).
Rudinger, G., "Effective Drag Coefficient for Gas-Particle Flow in Shock Tubes," *Trans. ASME*, **92D**, 165 (1970).
Schuyler, F. L., "Comment on 'Drag Coefficient of Small Spherical Particles," *AIAA J.*, **7**, 573 (1969).
Selberg, B. P., and J. A. Nicholls, "Drag Coefficient of Small Spherical Particles," *AIAA J.*, **6**, No. 3, 401 (1968).
Torobin, L. B., and W. H. Gauvin, "Fundamental Aspects of Solids-Gas Flow," *Can. J. Chem. Eng.*, Part I, **37**, 129 (1959); Part II, id. **37**, 167 (1959); Part III, id., **37**, 224 (1959); Part IV, id., **38**, 142 (1960); Part V, id., **38**, 189 (1960); Part VI, id., **39**, 113 (1961).
Wang, C. C., "Deceleration and Turbulence Effects on Sphere Drag Coefficient," M. Eng. Thesis, McGill University, Montreal, Canada (1969).
Wieselsberger, C., "Further Studies on the Laws of Fluids and Air Drag," *Physik. Zeit.*, **23**, 219 (1922).
Yoshizawa, A., "On the Mechanism of the Movement of a Separation Point," *J. Phys. Soc. Japan*, **39** (2), 509 (1975).

Manuscript received January 15, 1979; revision received May 2, and accepted May 7, 1979.

Measurement and Scale-Up of Secondary Nucleation Kinetics for the Potash Alum-Water System

JOHN GARSIDE

and

SLOBODAN J. JANČIĆ

**Department of Chemical and Biochemical Engineering
University College London
Torrington Place
London WC1E 7JE U.K.**

Secondary nucleation kinetics for potash alum in draft-tube baffled crystallizers have been determined from steady state crystal size distributions measured down to about 5 μm. Differences in nucleation rates were found for crystallizers of similar geometry but different capacity. Models relating the frequency of crystal/propeller collisions to crystallizer geometry and operating parameters were compared. In general, these successfully accounted for the observed differences in nucleation rates.

SCOPE

Nucleation rates in continuous crystallizers can be measured using the mixed suspension mixed product removal (MSMPR) concept (Randolph and Larson 1971). However, when the crystal growth rate is size-dependent in the range of sizes into which secondary nuclei are produced, the nucleation rate cannot be unambiguously calculated from the crystal size distribution (CSD) unless the size-dependent growth rate is determined by independent measurements. The first objective of the work reported here is to combine growth rates that had been measured previ-

Correspondence concerning this paper should be addressed to J. Garside. S. J. Jančić is now with Delft University of Technology, Laboratory for Process Equipment, Delft, Netherlands.

0001-1541-79-2923-0948-$01.25.